AD-A182 097 OKLAHOMA DOWNBURSTS AND THEIR ASYMMETRY(U) NATIONAL OCEANIC AND ATMOSPHERIC ADMINISTRATION NORMAN OK NATIONAL SEVERE STORMS LAB M D EILTS ET AL. NOV 86 1/1

UNCLASSIFIED DOT/FAA/PM-87/7 DTFA01-80-Y-10524 F/G 4/2 NL

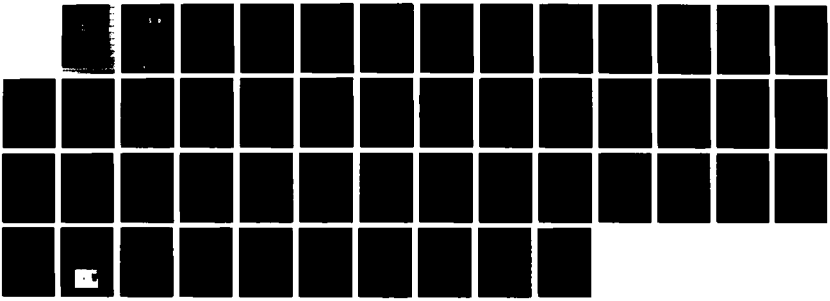

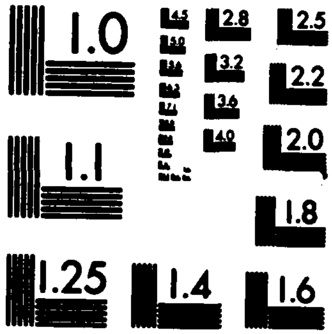

MICROCOPY RESOLUTION TEST CHART
NATIONAL BUREAU OF STANDARDS-1963-A

DOT/FAA/PM-87/7

Program Engineering
and Maintenance Service
Washington, D.C. 20591

Oklahoma Downbursts and Their Asymmetry

Michael D. Eilts
Richard J. Doviak

National Severe Storms Laboratory
1313 Halley Circle
Norman, OK 73096

November 1986

Final Report

This document is available to the public through the National Technical Information Service, Springfield, Virginia 22161.

U.S. Department of Transportation
Federal Aviation Administration

Technical Report Documentation Page

1. Report No. DOT/FAA/PM-87/7	2. Government Accession No. AD-A182 097	3. Recipient's Catalog No.
4. Title and Subtitle Oklahoma Downbursts and Their Asymmetry		5. Report Date November 1986
		6. Performing Organization Code MGG000
		8. Performing Organization Report No.
7. Author(s) Michael D. Eilts and Richard J. Doviak		
9. Performing Organization Name and Address National Severe Storms Laboratory 1313 Halley Circle Norman, OK 73069		10. Work Unit No. (TRAIS)
		11. Contract or Grant No. DTFA01-80-Y-10524
12. Sponsoring Agency Name and Address U.S. Department of Transportation Federal Aviation Administration Program Engineering and Maintenance Service Washington, D.C. 20591		13. Type of Report and Period Covered Final Report
		14. Sponsoring Agency Code APM-310
15. Supplementary Notes		

16. Abstract

Doppler radar data, collected each spring in 1979-1984, with the two Doppler radars operated by the National Severe Storms Laboratory (NSSL), are used to investigate the asymmetry of low-altitude divergent outflows of convective storm downbursts in central Oklahoma. Outflows in Oklahoma storms can be highly asymmetric with horizontal shear along the axis of maximum divergence as much as 5.5 times the shear along the axis of minimum divergence. The downbursts observed in central Oklahoma, all large-scale (4-10 km) events, were superposed with the maximum reflectivity core of the storms. However, scanning strategies may have precluded detection of smaller scale (< 4 km) microbursts. Typical downbursts observed during the Joint Airport Weather Studies (JAWS) Project were of smaller scale (< 4 km) and were often associated with little or no rain at the surface. The mechanisms for the initiation of the majority of JAWS microbursts was most likely evaporative cooling, which occurred when precipitation fell into a dry, deep and nearly adiabatic boundary layer; it appears that, because of a lower cloud base and a moister and slightly more stable boundary layer, the mechanisms for the initiation of the observed Oklahoma downbursts include low-level melting, as well as evaporation of precipitation, low-level precipitation loading, and evaporational cooling at middle levels due to entrainment of dry air.

17. Key Words downbursts, NEXRAD, wind shear	18. Distribution Statement This document is available to the public through the National Technical Information Service, Springfield, Virginia 22161.

19. Security Classif. (of this report)	20. Security Classif. (of this page)	21. No. of Pages	22. Price
UNCLASSIFIED	UNCLASSIFIED	48	

Form DOT F 1700.7 (8-72) Reproduction of completed page authorized

PREFACE

The authors would like to thank our colleagues at the National Severe Storms Laboratory for support and for the data sets on which tnis study was based. Appreciation is also extended to J.T. Dooley who photographed and cataloged the slides of the Doppler displays. Michelle Foster and Carole J. Holder typed the manuscript and Joan Kimpel and Robert Goldsmitn performed graphic services.

TABLE OF CONTENTS

LIST OF ILLUSTRATIONS

Fig. 4a. Dual Doppler vector wind field of 1522:30 CST, 19 May 1984, downburst case 2. Details are the same as in Fig. 3a except the radius of influence used in interpolation was 300 m.

Fig. 4b. Plot of maximum divergent radial velocity difference for downburst case 2 (see Fig. 3b).

Fig. 5a. Dual Doppler vector wind field of 2143:30 CST, 19 June 1980, downburst case 3. Details are the same as in Fig. 3a except that vectors are ground relative.

Fig. 5b. Plot of maximum divergent radial velocity difference for downburst case 3 (see Fig. 3b).

Fig. 6. Radial velocity contours for a fictitious radar located at 150°/15 km from the center of downburst case 1. Note the large divergent radial velocity difference along the radial between the radar and the center of the downburst (marked by *).

Fig. 7. Radial velocity contours for a fictitious radar located at 60°/15 km from the center of downburst case 1. Note the very little divergent radial velocity difference along the radial between the radar and the center of the downburst.

Fig. 8. Typical sounding for high-based, shallow-depth clouds that are associated with "dry" microbursts. Sounding is for 14 July 1982 at 2300 GMT from Denver, Colorado. (Figure courtesy of J. McCarthy, National Center for Atmospheric Research/National Science Foundation. From McCarthy and Wilson, 1984.)

Fig. 9. Sounding for a heavily precipitating thunderstorm that produced a microburst. Sounding is for 23 June 1982 at 2325 GMT from Denver, Colorado. (Figure courtesy of J. McCarthy, National Center for Atmospheric Research/National Science Foundation. From McCarthy and Wilson, 1984.)

Fig. 10. Typical sounding of an Oklahoma thunderstorm environment. Sounding is for 27 May 1984 at 1330 CST from Edmond, Oklahoma. Downburst case 1 occurred on this day.

LIST OF ILLUSTRATIONS

Appendix B

LIST OF ILLUSTRATIONS

Appendix C

LIST OF TABLES

1. Introduction

This study of intense, thunderstorm-related downdrafts in Oklahoma extends previous studies of the same phenomenon in Illinois and Colorado. Project NIMROD (Northern Illinois Meteorological Research on Downbursts) was the first study designed to collect data on downbursts, defined by Fujita (1981) as a "strong downdraft which induces an outburst of damaging winds on or near the ground." In this study the definition of a downburst is modified in accordance with Wilson et al. (1984) to that of a Doppler-radar-observed divergent outflow near the surface with differential Doppler velocity across the divergence center of at least 10 m s^{-1}. Further, downbursts are called microbursts when they are 0.4-4 km in diameter, and macrobursts when they are greater than 4 km in diameter (Fujita and Wakimoto, 1983). The NIMROD Doppler radar network was too coarse to obtain high-resolution multi-radar information, but single Doppler data were collected on several microburst events (Fujita and Wakimoto, 1983). On the basis of knowledge obtained from NIMROD, the Joint Airport Weather Studies (JAWS) project was organized to collect high resolution data on downbursts. JAWS utilized three Doppler radars located in a small triangle centered near Denver's Stapleton International Airport as well as a dense network of 27 Portable Automated Mesonet (PAM) stations located in the area of multiple Doppler coverage so that the three-dimensional wind field of microbursts could be determined (McCarthy et al., 1982).

Some major discoveries were made during JAWS.

(1) There were more microbursts, at least in the Denver area, than had been expected. During the 83 days of the JAWS observation there were 49 days in which at least one microburst was detected, and 186 microbursts were identified by the PAM network on these 49 days (~70 were identified by Doppler radar). Furthermore, 151 of the 186 microbursts (81%) were dry microbursts; that is, little or no rain fell during the event (Fujita and Wakimoto, 1983).

(2) There was no correlation between radar reflectivity of the parent cell and strength of the Denver microbursts (Wilson et al., 1984).

(3) Microbursts observed during JAWS were asymmetric; the shear along the maximum shear axis was sometimes as much as 6 times the shear along the minimum shear axis (Wilson et al., 1984).

(4) The radial velocity difference across the average microburst in the Denver area, as measured by Doppler radar, was 12 m s^{-1} initially over 1.8 km in range. Within 5 minutes of the initial observed divergence pattern, 50% of all microbursts had reached their maximum velocity difference. At the time of maximum velocity difference the average microburst had strengthened to show a velocity difference of 24 m s^{-1} over a distance of 3.1 km (Wilson et al., 1984), which is approximately the same shear as the initial observance but over a larger distance.

Low-level wind shear has been implicated in a number of aircraft accidents (National Research Council, 1983). The downburst is dangerous because of its small scale and strong divergence. An aircraft encountering a downburst while landing or taking off initially gains airspeed and then suddenly loses airspeed, which is especially dangerous near the ground (Fig. 1) (Wilson et al., 1984). Frost (1983), using numerical studies of flight in thunderstorm-type wind shear, showed that a combination of downdraft and horizontal longitudinal shear over a distance that corresponds to the aircraft's phugoid frequency can cause a large deviation from the intended flight path. Thus, horizontal longitudinal shear on the scale of 1-4 km is the most critical to aircraft performance (McCarthy and Norviel, 1982). That scale is precisely the size of the shear resulting from downbursts from convective storms.

The next-generation weather radar system (NEXRAD), which is being developed under a joint program by the Federal Aviation Administration (FAA), the

National Weather Service (NWS), and the U.S. Air Force Air Weather Service (AWS), could be used to detect low-altitude wind shear in the terminal area of airports (Mahapatra and Lee, 1984). The main task of this Doppler radar would be to estimate the wind shear along each runway in the terminal area. The siting of such a Doppler radar to perform this task is being debated at length.

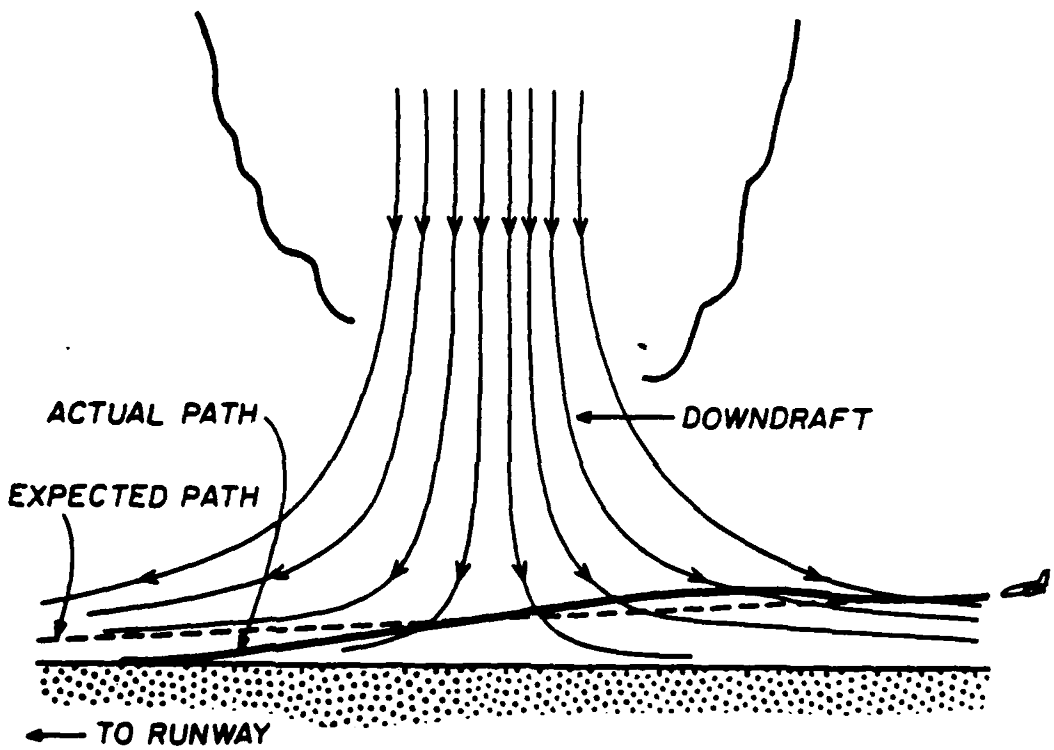

Fig. 1. Effect of a downdraft on the flight of an aircraft penetrating the downdraft. Initially the aircraft experiences increasing headwinds, then downdraft, and finally a strong tailwind that could cause the aircraft to drop below its expected path enough to cause impact with the ground.

Mahapatra et al. (1983) concluded that if a single Doppler radar has to detect all hazardous convective phenomena over the entire terminal area, the optimum Doppler radar site is 10-12 km from the center of the runway complex. An off-airport site would allow the Doppler radar to detect precursors to downbursts over the terminal area and to estimate shears along each runway path if detected downbursts are symmetric or if they are predictably asymmetric. An on-airport site would create problems such as an overhead blind zone, ground clutter in the area of interest, and difficulty in locating a site on the runway complex.

On the other hand, Wilson et al. (1984) pointed out that an off-airport site would not be able to measure shear directly along each runway as could a radar placed at the center of a runway complex. Although an off-airport radar is able to detect a downburst or gust front and locate it with respect to intended flight paths it cannot provide a direct measurement of longitudinal shear for all approaches because the magnitude of the shear may be dependent on the viewing angle of the radar. For 13 microbursts studied using the JAWS data, the average microburst had shear twice as strong along the maximum shear axis compared with the shear along the minimum shear axis. In some cases shear was 6 times as strong along the maximum shear axis as it was along the minimum shear axis. Thus, a single Doppler radar, placed at an off-airport site not parallel to an intended flight path, may underestimate shear along that flight path by a factor of 6, unless suitable algorithms are developed to estimate the actual shear reliably from the volume of Doppler spectral moment data (i.e., velocity, reflectivity and spectral width).

Owing to the limitations of single Doppler radars, Wilson et al. (1984) proposed that two Doppler radars be placed near each airport so that the three-dimensional vector windfield in the entire terminal area could be resolved, and shear for any intended flight path could be determined. However, the initial cost of placing two Doppler radars at each airport may be prohibitive.

The study presented here examines the characteristics of downbursts in Oklahoma thunderstorms with emphasis on asymmetries in low-altitude divergent outflows. Determining the asymmetry of low-altitude divergent outflows is important for ascertaining whether a single Doppler radar, sited near an airport, could reliably detect wind shear that may be hazardous to aircraft. The existing data base of the two National Severe Storms Laboratory's (NSSL) Doppler radars was used to investigate the horizontal structure of downbursts at low altitudes.

2. Data

Each spring NSSL conducts an observational program in which dual Doppler radar data are collected. The two Doppler radars are located ~41 km apart, one in Norman (NRO) and the other at Page (formerly Cimarron) airfield in Oklahoma City (CIM) (Fig. 2). Most often radar data are collected simultaneously by both radars, starting at elevation angle 0.5° and completing a full tilt sequence through a storm using a sector scan of ~60° and vertical resolution of 0.5°-1.0°. A tilt sequence is usually repeated every 5-10 minutes. The main objective of data collection is to obtain information on large convective storms that cause severe weather (hail, damaging winds, tornadoes, etc). Thus, smaller scale storms that may have caused microbursts were not scanned on a regular basis. For this reason, most of the storm outflows investigated in this study are larger-scale downbursts (macrobursts) that were imbedded in large intense convective storms. This does not suggest that microbursts such as those identified during JAWS do not occur in Oklahoma;

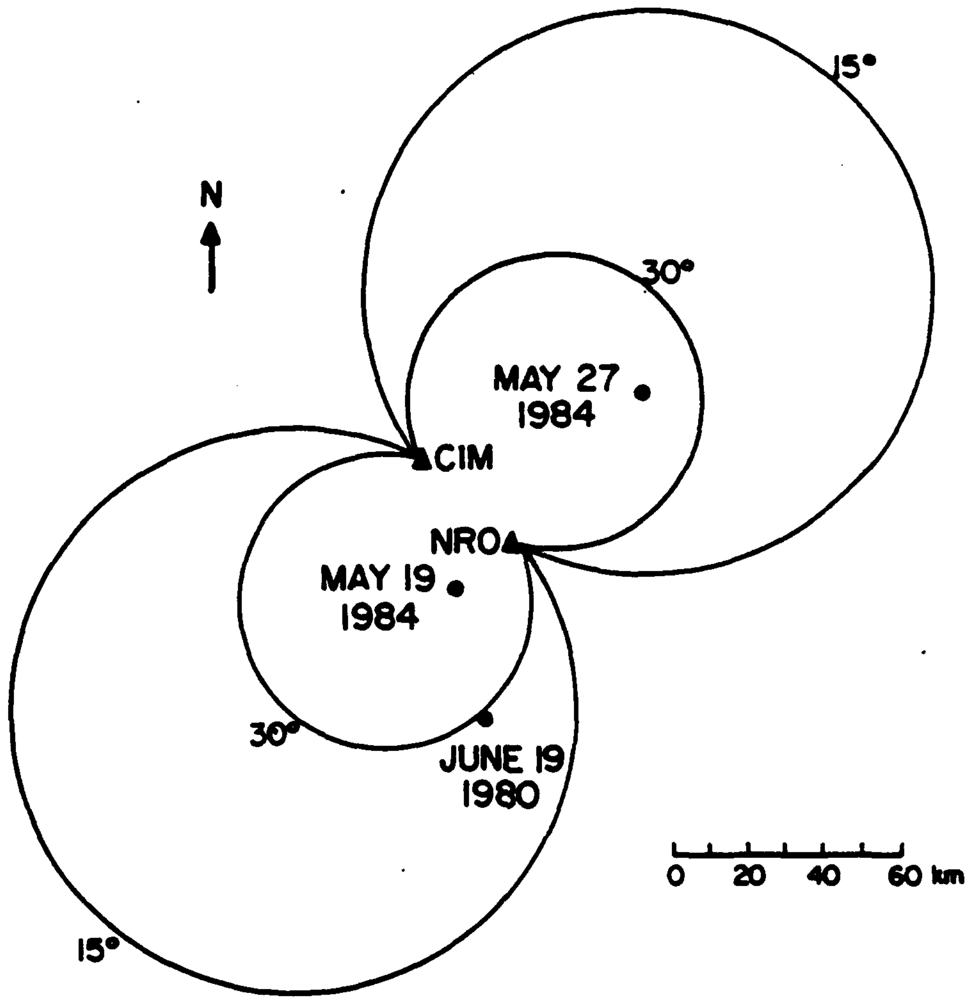

Fig. 2. Location of the two Doppler radars, area of dual Doppler coverage (the angles are the angles between the radar beams), and locations of the three downbursts investigated in this study.

rather the scanning strategies used with the NSSL Doppler radars may not have allowed the detection of such microbursts. We note, however, that climatological differences may hinder the "dry microbursts" observed during JAWS from occurring in Oklahoma. (This is discussed in Section 5.)

3. Data Analysis

An initial search for possible low-altitude divergent outflows was conducted by looking through spring program summaries, radar logs, etc. for the 6-year period 1979-1984. During this period, dual Doppler radar data were collected on 39 days. Of these 39 days, 30 were selected for further examination. All the 1983 and 1984 cases (15) were examined because the data were easily viewed on color slides, which had been taken of the Doppler velocity field for each low-level elevation angle scan of the Norman Doppler radar. From the years 1979-1982, 15 days were selected by identifying which days low-altitude divergence or large radial velocities were noted in the radar logs, or straight-line wind damage was reported in the spring program summary; other days were also included if there was any possibility of strong low-altitude outflow. The days that were not selected were typically weakening squall lines (with associated weakening gust front) as they approached the dual Doppler area, or weak thundershowers imbedded within a large area of rain. The 15 days of single Doppler radar data from 1979-1982 were viewed on the color display. From the 15 days in the years 1979-1982 and from the 15 days in 1983 and 1984, nine possible low-altitude divergent outflows were identified and singled out for dual Doppler analysis. Note that downbursts associated with mesocyclones were excluded from this study because the identifiability of mesocyclones with Doppler radar and their dangers to aircraft have already been reported (Lemon et al., 1977).

Before dual-Doppler analysis was initiated the Doppler velocity data were edited using a local environmental check algorithm. This algorithm is described in Appendix A. Briefly, the algorithm compares the velocity value in question with nine neighboring points in the same and in the preceding adjacent radial. If the velocity value is not within a band determined by statistical properties of the nine neighboring points an attempt is made to dealias it into this band; if this cannot be done the velocity value is removed. After editing, the single Doppler radar data were interpolated to commonly located grids using a Cressman weight (Cressman, 1959) with horizontal radius of influence of 300-700 m, depending on the distance from the radar to the grid. No vertical interpolation was necessary because only the lowest elevation angle scan was used ($\theta_e = 0.5°$ for 1980-1983, and $\theta_e = 0.0°$ for 1984). Dual Doppler analysis was completed using the multiple Doppler radar analysis system described by Brown et al. (1981).

Of the nine cases selected initially for dual Doppler analysis, six were not used because of bad data from one of the radars, or non-simultaneous data collection at the necessary time, or because one of the radars did not detect the low-altitude divergence due to the height of the radar beam in the area of the downburst. Details on the three downbursts finally studied for symmetry are given in Table 1.

Table 1: Downbursts Used for the Symmetry Study

Case	Date	Time of Maximum Shear	Maximum Reflectivity	Maximum Velocity Difference	Distance Between Max. Vel. Difference
1	27 May 1984	1630:00 CST	50 dBZ	22 m s^{-1}	4.0 km
2	19 May 1984	1522:30	40	16	5.0
3	19 June 1980	2143:30	60	36	8.0

The horizontal windfield at the lowest observed altitude is shown for each of these downbursts in Figs. 3a, 4a and 5a. The mean wind, which is an average over the data field, has been subtracted from Figs. 3a and 4a to show the perturbation wind so that the divergent flow is more easily noticed. More information on the three downbursts is given in Appendix B.

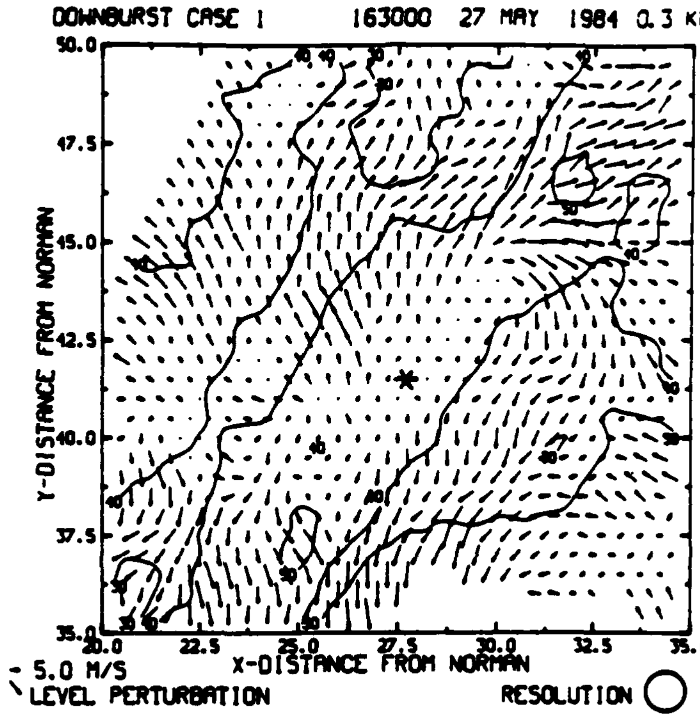

Fig. 3a. Dual Doppler perturbation wind field of 1630:00 CST, 27 May 1984 downburst case 1. Grid size is 15 km x 15 km (dx = dy = 250 m). A horizontal radius of influence of 500 m was used in a Cressman weighting scheme. The average wind vector of the data field has been removed to show the divergent outflow. Contours are reflectivity factor in dBZ. The star (*) indicates the location chosen as the center of the outflow for later analysis. The resolution, as indicated by the circle in the lower right hand corner, is the area from which data were interpolated to each grid point.

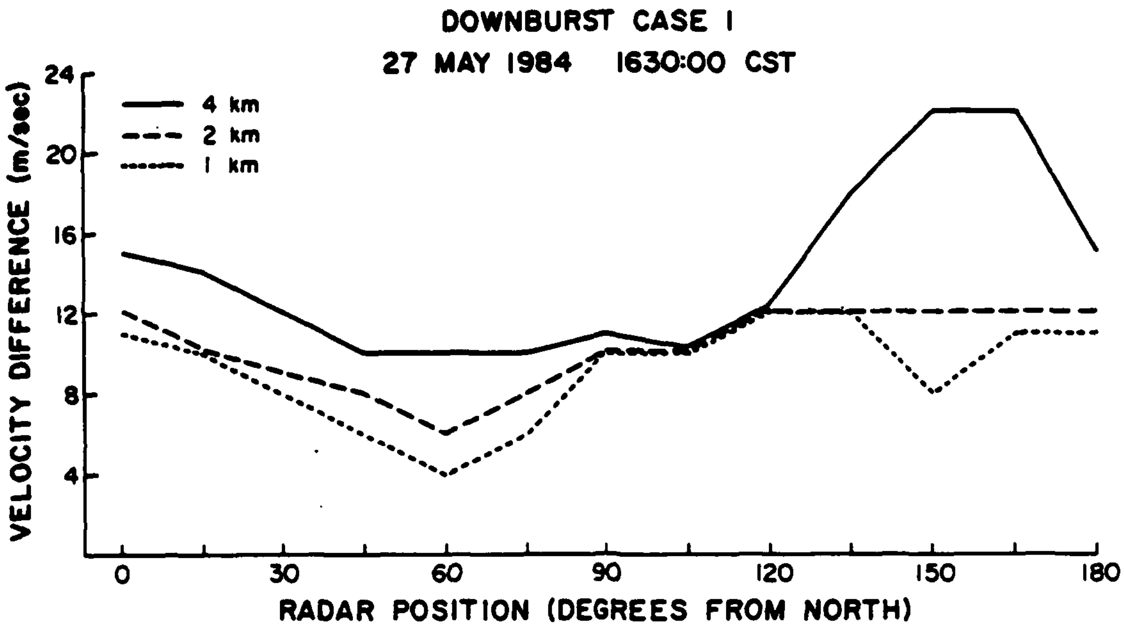

Fig. 3b. Plot of maximum divergent radial velocity difference over the distances 1 km, 2 km, and 4 km for downburst case 1. Radar position is the angle clockwise from North of a fictitious radar which was placed 15 km from the center of the downburst.

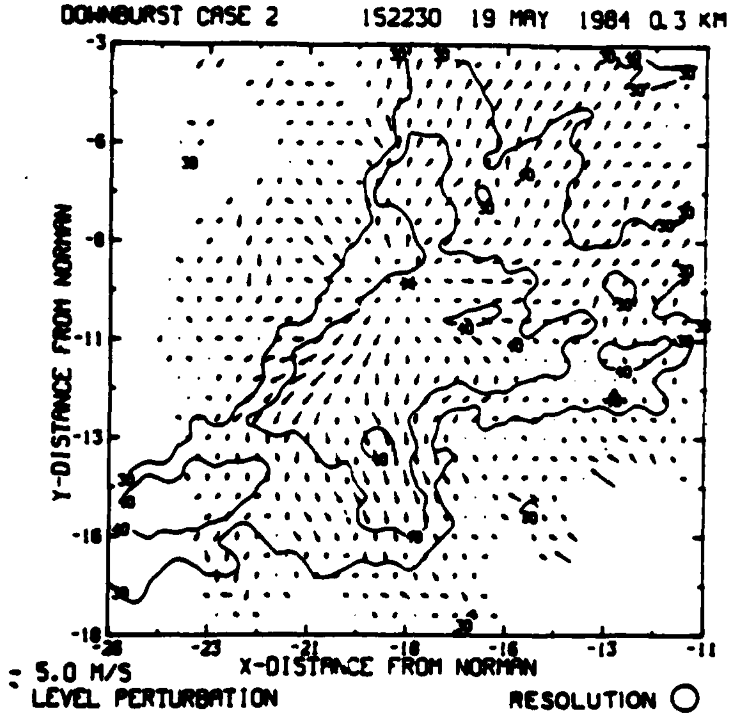

Fig. 4a. Dual Doppler vector wind field of 1522:30 CST, 19 May 1984, downburst case 2. Details are the same as in Fig. 3a except the radius of influence used in interpolation was 300 m.

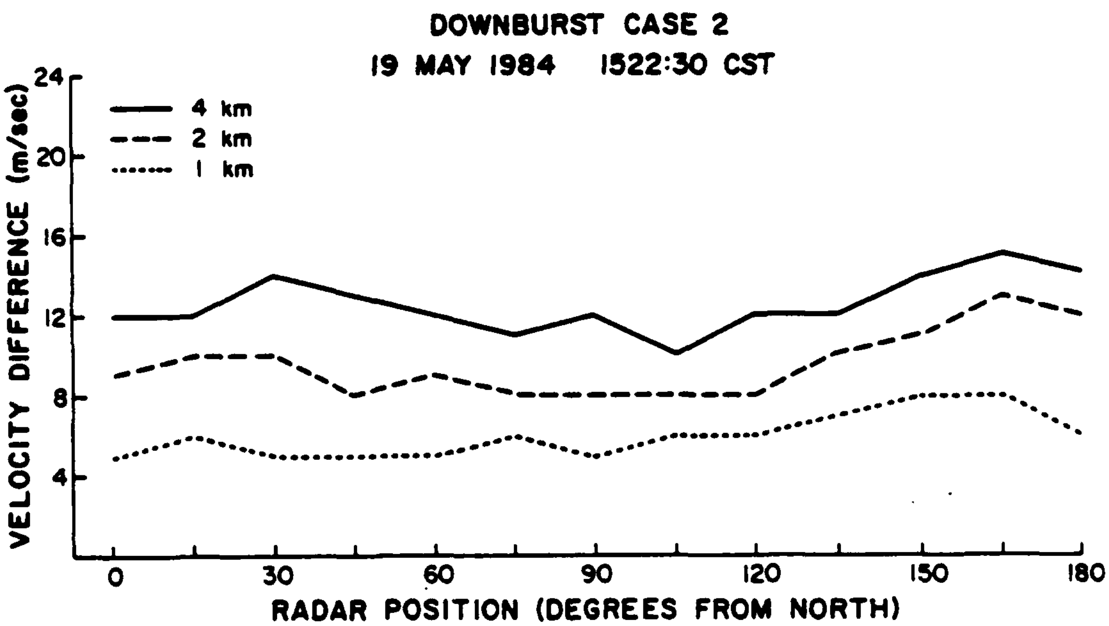

Fig. 4b. Plot of maximum divergent radial velocity difference for downburst case 2 (see Fig. 3b).

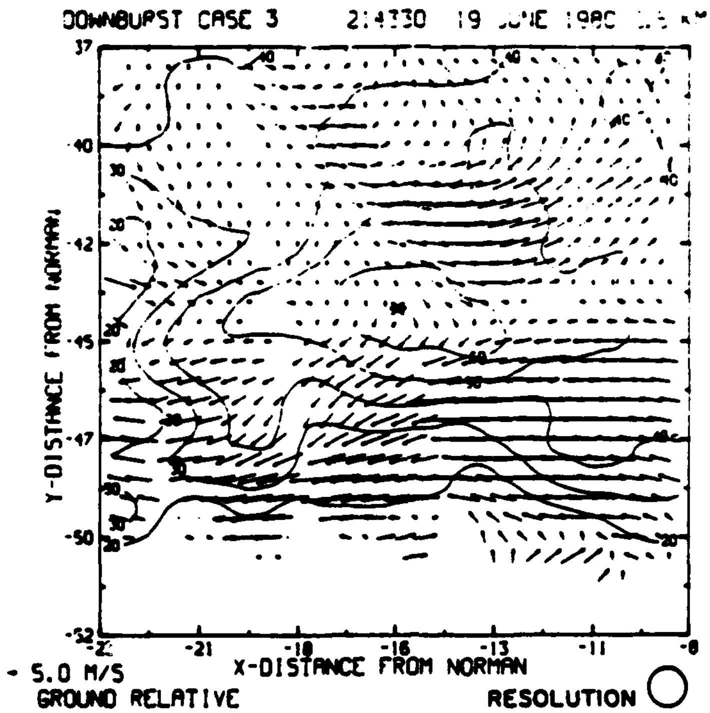

Fig. 5a. Dual Doppler vector wind field of 2143:30 CST, 19 June 1980, downburst case 3. Details are the same as in Fig. 3a except that vectors are ground relative.

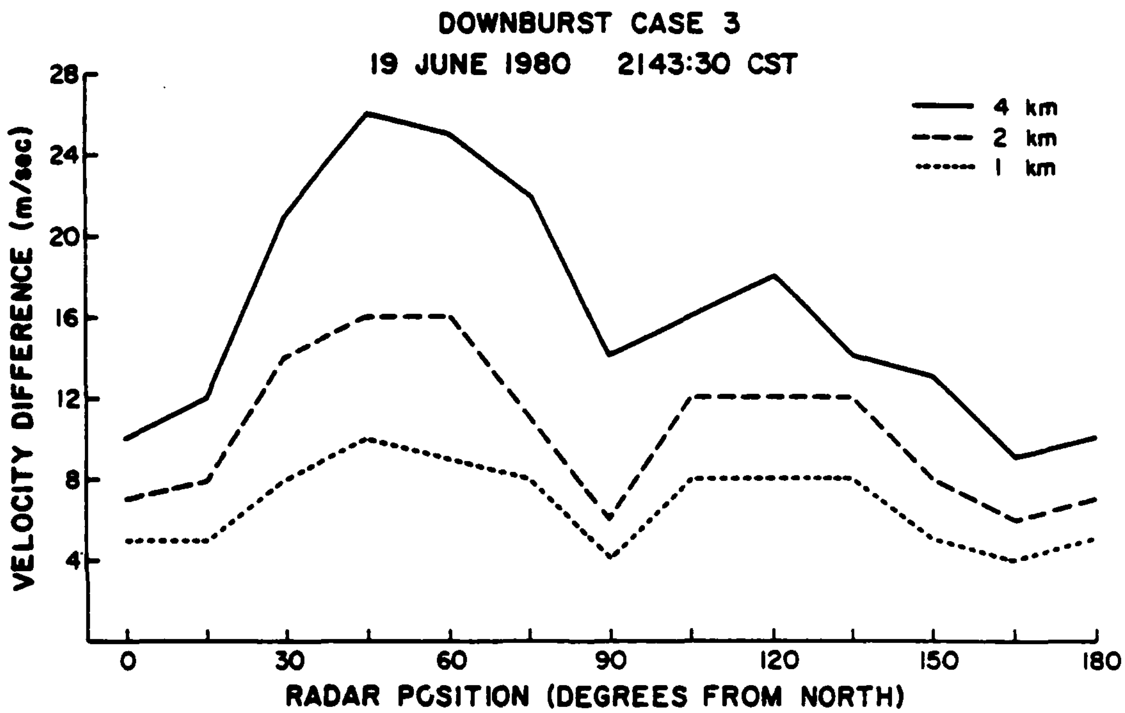

Fig. 5b. Plot of maximum divergent radial velocity difference for downburst case 3 (see Fig. 3b).

4. Symmetry of the Low-Altitude Divergent Outflow

To investigate the symmetry of the low-altitude divergent outflows shown in Figs. 3a, 4a and 5a we placed a fictitious radar at 15 km range from the center of each outflow (indicated by a * in the figures) at 15° intervals from 0°-180°. We calculated the radial velocity toward or away from the fictitious radars at each grid point, using the dual Doppler wind fields. Then the maximum divergent radial velocity difference across the distances 1, 2, and 4 km were determined for each angle. This is the distance (1-4 km) over which low-altitude shear is most critical to aircraft performance (McCarthy and Norviel, 1982).

In Figs. 3b, 4b and 5b, maximum divergent radial velocity differences over the three distances are plotted vs. angle of the fictitious radar from the center of the outflow for each of the three downburst cases. It is evident that all three cases investigated here are asymmetric.

Table 2 shows the ratio of maximum shear to minimum shear for the three downburst cases over the distances 1, 2, and 4 km.

Table 2: Ratio of Maximum Shear to Minimum Shear

Case	Date	Distance	$\frac{\Delta V_{max}}{\Delta V_{min}}$
1	27 May 1984	1 km	3.0
		2	2.0
		4	2.2
2	19 May 1984	1 km	1.6
		2	1.6
		4	1.5
3	19 June 1980	1 km	2.5
		2	2.7
		4	2.9

To show the difference that the viewing angle of the radar makes in the estimated shear we will look more closely at the 27 May 1984, downburst case. This downburst occurred in a line of thunderstorms that produced several downbursts on this day and a strong gust front in the central Oklahoma area. As is seen in Fig. 3a this downburst was elongated (10 km x 5 km) and the winds curved anticyclonically out from the line of divergence. From Fig. 3b we can see that the maximum divergence is observed when a radar is placed at 150° from the center of this downburst and the minimum when the radar is at 60° from the center. Figures 6 and 7 show contours of the radial velocity field from these two positions. There is a remarkable difference between the two fields. Figure 6 depicts a line of divergence, whereas in Fig. 7 azimuthal shear is most noticeable, indicative of moderate anticyclonic shear. Radial velocity gradients are also weaker in Fig. 7.

In Fig. 6, two centers of strongest divergence can be identified, one centered at (27, 41), which is near the center of the downburst, and the other at (31, 45), which is on the northeast edge of the downburst. The shear values shown in Table 2 are values representative of the whole downburst; i.e., shears from both divergent centers contributed to the maximum and minimum shears. However, if we look, at the individual centers of divergence we see that the shear at the center of the downburst is highly asymmetric; i.e., a radar located at 60° from the downburst would detect a divergent velocity difference of only 4 m s^{-1} through the center of the downburst, but a radar located at 150° from the center would observe a divergent velocity difference of 22 m s^{-1}. This is a ratio of 5.5:1, similar to the most asymmetric cases observed during JAWS. This could be a particularly dangerous situation for aircraft. If a radar were located at 60° from a downburst such as this, the radial velocity field would liik fairly benign to a radar interpreter because

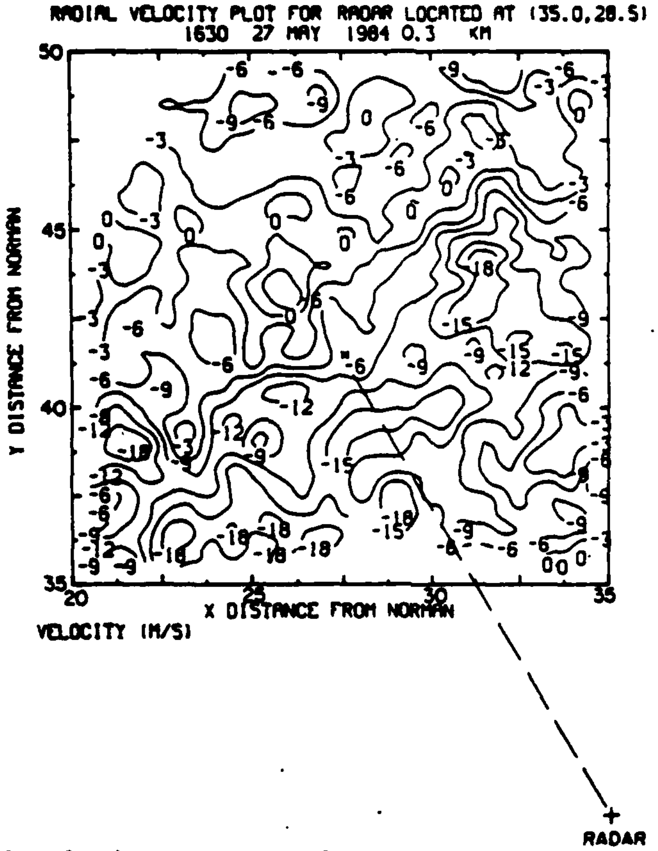

Fig. 6. Radial velocity contours for a fictitious radar located at 150°/15 km from the center of downburst case 1. Note the large divergent radial velocity difference along the radial between the radar and the center of the downburst (marked by *).

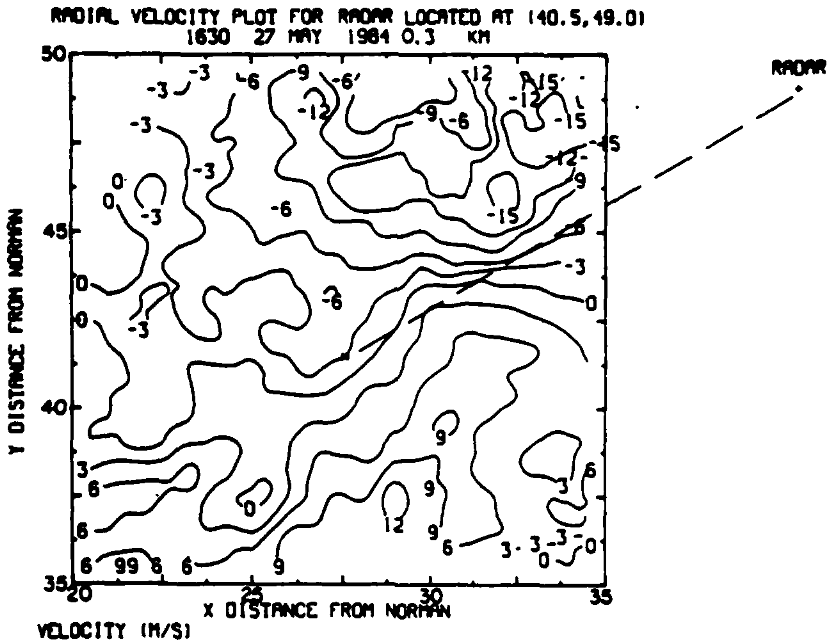

Fig. 7. Radial velocity contours for a fictitious radar located at 60°/15 km from the center of downburst case 1. Note the very little divergent radial velocity difference along the radial between the radar and the center of the downburst.

of the weak radial velocity gradients and very little divergence. However, the actual wind field is strongly divergent and could be dangerous to aircraft penetrating it.

5. Discussion

The downbursts observed with NSSL's two Doppler radars in central Oklahoma are different from typical downbursts observed during JAWS. Of the 186 microbursts detected by the surface stations during JAWS, only 31 had any rain associated with them and only 13 had more than 0.05 inches associated with them (Fujita, 1985), on the other hand, the observed Oklahoma downbursts were imbedded within intense convective storms.

A typical sounding for high-based, shallow-depth clouds associated with light rain or virga-produced microbursts is shown in Fig. 8. This sounding was taken on July 14, 1982 at 2300 GMT from Denver, Colorado, on a day in which several dry microbursts were observed in the JAWS observation area. The sounding conducive to "dry microbursts" is characterized by a deep (3-4 km), very dry boundary layer, with a nearly dry adiabatic lapse rate of temperature, and a moist layer at or near 500 mb (McCarthy and Wilson, 1984).

The other type of microburst observed during JAWS was associated with heavily precipitating thunderstorms. A sounding for a heavily precipitating thunderstorm environment that produced a microburst is shown in Fig. 9. Again the sounding is characterized by a dry, near adiabatic boundary layer. However, the middle-level moisture is much deeper, allowing the growth of deep clouds that produce heavy precipitation.

Using a one-dimensional time dependent model of an evaporatively driven downdraft, Srivastava (1985) showed that for typical summertime conditions in Colorado, intense microbursts should develop near the ground as the lapse rate

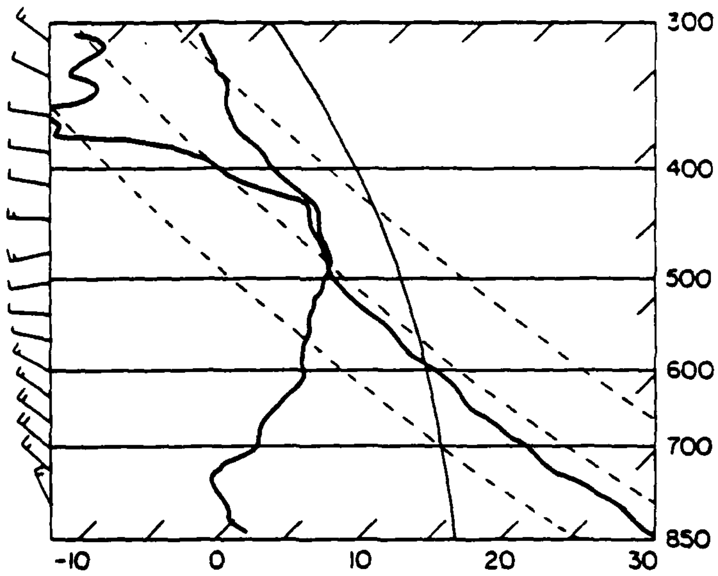

Fig. 8. Typical sounding for high-based, shallow-depth clouds that are associated with "dry" microbursts. Sounding is for 14 July 1982 at 2300 GMT from Denver, Colorado. (Figure courtesy of J. McCarthy, National Center for Atmospheric Research/National Science Foundation. From McCarthy and Wilson, 1984.)

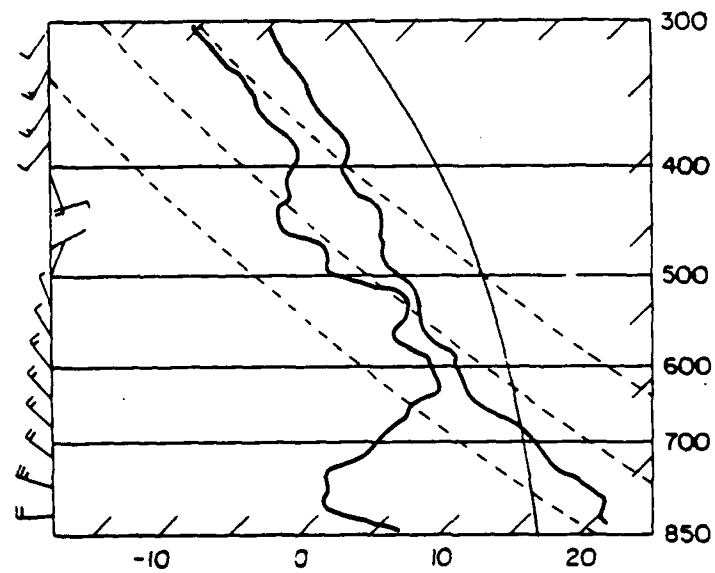

Fig. 9. Sounding for a heavily precipitating thunderstorm that produced a microburst. Sounding is for 23 June 1982 at 2325 GMT from Denver, Colorado. (Figure courtesy of J. McCarthy, National Center for Atmospheric Research/National Science Foundation. From McCarthy and Wilson, 1984.)

of temperature in the sub-cloud layer approaches the dry adiabatic rate, and as the rainwater mixing ratio at cloud base increases. Observations from JAWS confirm the model results. During JAWS the frequency of microbursts increased significantly as the lapse rate approached the dry adiabatic rate. As the lapse rate became more stable, microbursts tended to occur only for relatively higher values of rainwater mixing ratio (reflectivity). Thus Srivastava concluded that "a majority of microbursts observed in the JAWS project was probably driven solely by evaporative cooling." Since the forcing at cloud base was kept to a minimum in his model, all the forcing occurred because of evaporative cooling below cloud base.

Downbursts observed in Central Oklahoma and Colorado occur in quite different kinds of environments. A sounding taken on a day when downbursts were observed in Central Oklahoma is shown in Fig. 10. This sounding was taken from Edmond, Oklahoma, at 1330 CST on 27 May 1984, the day that downburst case 1 occurred. Numerous reports of straight line wind damage were given on this day (NOAA, 1984). Typical soundings such as this one are characterized by a relatively shallow boundary layer (1-2 km), which is moist with a layer of dry air overlying the boundary layer. Typical cloud base of Oklahoma thunderstorms is ~1 km above ground level.

There are three main reasons to believe that evaporative cooling below cloud base is not a significant factor in producing downbursts within intense convective storms in central Oklahoma:

(1) There is a relatively lower cloud base, which allows less time for parcel acceleration.

(2) The sub-cloud layer is relatively moist, which decreases the rate of evaporation.

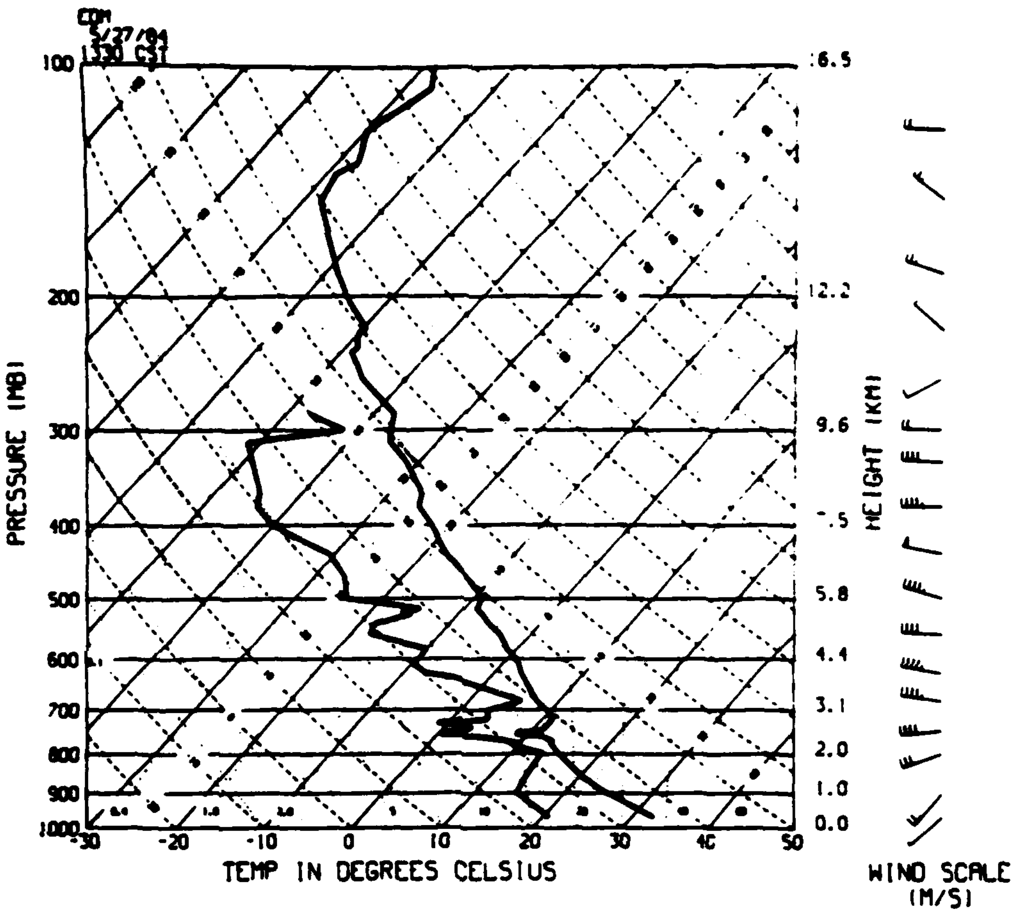

Fig. 10. Typical sounding of an Oklahoma thunderstorm environment. Sounding is for 27 May 1984 at 1330 CST from Edmond, Oklahoma. Downburst case 1 occurred on this day.

(3) There is a slightly more stable lapse rate of temperature in the lower troposphere (Darkow, 1969), which was shown by Srivastava (1985) to be a critical factor.

Results from this study support numerous other studies (e.g., Lemon and Doswell, 1979) in determining that two main types of intense downdrafts (downbursts) occur within large, intense convective storms in Oklahoma: (1) divergent outflows that are superposed with the maximum reflectivity core of a storm, as in the three cases presented in this report, and (2) downbursts associated with low-level mesoscale circulations.

The first of these is related to the thunderstorm downdraft that occurs in every thunderstorm but by definition is of greater magnitude. A number of studies have been done on the thunderstorm downdraft, some of them which have shown conditions for the production of intense downdrafts. Some of these studies are summarized below.

The first comprehensive study on the downdraft from convective storms was done by Byers and Brahm (1949), using data collected during the Thunderstorm Project. They attributed the initiation of the downdraft to precipitation drag and maintenance of it to evaporational cooling. Kamburova and Ludlam (1966) modeled precipitation-associated downdrafts, using a one-dimensional, steady-state, kinematic model. They found that general conditions for the production of strong downdrafts are a lapse rate close to the dry adiabatic rate from the ground to the middle troposphere, and intense rainfall. The rainfall contributed to downdraft production from both drag forces and evaporational cooling. Evaporational cooling was found to be dependent on the size and intensity of the precipitation.

A more sophisticated one-dimensional, time-dependent model which included entrainment and updraft-downdraft interaction effects was used by Haman and

Niewiadomski (1980) to show that conditions for strongest downdrafts include moderate instability, low humidity, and entrainment of environmental air into both the updraft and downdraft.

In a more recent comprehensive study on downdrafts from convective storms (Knupp, 1985) both observations (multi-Doppler radar data) and a cloud model were used. Results from this study showed that the strength of low-altitude downdrafts associated with the precipitation core depends on the size and intensity of the precipitation, environmental dryness and stability at middle troposphere levels, and planetary boundary layer depth and stability. The main forcing for the precipitation-associated downdraft is low-altitude melting and evaporation of precipitation. Evaporational cooling at middle-tropospheric levels due to entrainment of dry air, and precipitation loading at low altitudes, appear to provide only secondary forcing. Furthermore, Knupp (1985) states that for a shallow boundary layer, such as that observed in Oklahoma, "melting of ice-phase precipitation represents the primary cooling source and therefore serves as a primary downdraft initiation mechanism." This precipitation-associated downdraft can attain relatively large scales, on the order of the horizontal dimensions of the low-level precipitation region. Such large scales are typical of the downbursts presented in this report, and other low-level outflows observed in Oklahoma (e.g., Klingle, 1985; Zrnic' and Lee, 1983).

A possible explanation for smaller scale downbursts that may occur in Oklahoma is the "penetrative downdraft" (Emanuel, 1981). When dry, potentially cold air, which is systematically entrained at middle levels of storms (Klemp and Wilhemson, 1978; Marwitz, 1972), becomes superposed over cloudy air, which has very high liquid water content, a highly unstable condition for "penetrative downdrafts" exists. This instability can be released when the cloudy air loses its upward velocity because of precipitation effects (loading or cooling), or because of dynamically induced vertical pressure gradients. Thus these small-scale downbursts may be produced when a penetrative downdraft forms at middle levels over a larger scale, possibly weaker, low-altitude precipitation associated downdraft.

The second type of downburst observed in Oklahoma, which was not in the scope of this study, is the downburst associated with low-altitude mesoscale circulations. An example of this type of downburst is reported by Wolfson (1983) and modeled by Klemp and Rotunno (1983). Both of these works describe downbursts associated with strong near-surface circulations; however, Wolfson's is for a stronger cell in a line of cells (the type often associated with a bow echo [Fujita, 1978]), and Klemp and Rotunno's is for a supercell. In both cases, it is believed that the low-altitude circulation increases as the gust front occludes and a strong small-scale downdraft (called an occlusion downdraft by Klemp and Rotunno) forms directly behind the gust front. It has been proposed that this occlusion process and its associated downburst are dynamically induced by the strong low-level rotation. The rotation induces low pressure coincident with the center of circulation and dynamically forces air down from above. In fact, in Klemp and Rotunno's (1983) model the downburst actually forms first at low altitudes and then extends upward as the flow adjusts to the vertical pressure gradients.

Aerial damage surveys done by Forbes and Wakimoto (1983) and Wakimoto (1983) support Klemp and Rotunno's (1983) model prediction that downbursts and tornadoes may coexist at low altitudes within a larger scale mesocyclonic circulation.

One other note should be made as to the difficulty of collecting good dual Doppler radar data on downbursts in Oklahoma. During this study many cases of possible downbursts were investigated and eventually ruled out for dual Doppler analysis. Two causes were most frequent:

(1) Coverage by one of the radars (or both) was lacking at the time of the downburst. This difficulty arises from to the varied nature of the research carried out at NSSL, and from all of the constraints this puts on scanning strategies of the two radars during data collection.

(2) One of the radars did not detect the low-altitude divergence associated with the downburst. This occurs even when a downburst is located in what is considered a good dual Doppler area. It happens because the strongest divergence associated with some downbursts is found in the lowest 500 m of the atmosphere. When the elevation angle is 0.5°, which was typically the lowest angle used during data collection in 1980-1983, the main power of the radar beam is above 500 m at ranges greater than ~60 km. Since 1984 the lowest elevation angle used for data collection with the NSSL radars has been 0.0°; this angle should extend somewhat the range at which low-level phenomena can be observed if the beam is not blocked and ground reflection does not distort the beam. An example of a strong downburst that was identified by the CIM radar but not by the NRO radar is shown in Appendix C.

It is evident that for dual Doppler radar data to be collected on a number of downburst cases in Oklahoma a specific study on downbursts would be required. However, even this might not guarantee numerous downburst cases within dual Doppler range because limiting observations to storms within 60 km of both radars means that a downburst must occur within a 4400 km^2 area, which is only about one-fifth the area considered adequate for dual Doppler coverage with the NSSL radars (Davies-Jones, 1979). Because of climatological differences between the JAWS observation area and other areas (e.g., Memphis [Wolfson et al., 1984]) where numerous microbursts have been identified and central

Oklahoma, where storms occur within radar range approximately every third day in the spring, opportunities to collect dual Doppler radar data on downbursts in Oklahoma are fewer. Each year during NSSL's spring program ~25 hours of dual Doppler data are collected; this leaves only about 5-10 hours of data collection each year in the area where both radars are able to detect low-altitude phenomena. Considering the short life span of downbursts (5-20 min) it is probable that few cases will occur in the small area needed for dual Doppler coverage of low-altitude divergence each year. In the spring of 1986, NSSL conducted an experiment to collect data on downbursts by collecting data on convection (not just severe) that occurred within 60 km of either of the two radars. This experiment, which was conducted in April, May, and June, should help determine the extent of the downburst hazard in the Oklahoma area.

6. Conclusions

Results from this study indicate that, because of climatological differences, typical downbursts observed in central Oklahoma are quite different than those that were observed around Denver, Colorado, during JAWS. The majority of microbursts observed during JAWS were probably driven by evaporative cooling below cloud base, which occurred when precipitation fell into a deep, dry, nearly adiabatic boundary layer. Lower cloud bases and a moister and slightly more stable boundary layer reduce the incidence of "dry" microbursts in the Oklahoma area. The downbursts observed in this study were associated with intense convective storms and were generally of much larger horizontal scale (macrobursts). However, due to scanning strategies used during data collection with the two NSSL Doppler radars, smaller scale microbursts that occurred may not have been scanned.

Initiation mechanisms for the downbursts observed probably include low-altitude melting and evaporation of precipitation, precipitation loading at low altitudes, and evaporational cooling at middle-tropospheric levels due to entrainment of dry air. Smaller scale microbursts may reach the ground when penetrative downdrafts (Emanuel, 1981), which form at middle-tropospheric levels, are superposed over a low-altitude downdraft. However, because of coarse surface data and inadequate time resolution in the Doppler data we were not able to verify the existence of these smaller scale events or to determine whether or not the macrobursts observed were intially of smaller scale.

The three downburst cases depicted indicate that low-altitude divergent outflows from convective storms in Oklahoma, as in Denver, can be highly asymmetric. Implications are that great care must be taken when placing radars near airports to detect low-altitude shears. If a single Doppler radar is not parallel to an intended flight path it may underestimate the shear along that intended flight path by as much as a factor of <u>six</u>. It if becomes necessary to portray the three-dimensional vector wind field in the entire terminal area, two Doppler radars near the airport may be required. Because of the large heavy rain cores associated with the downbursts observed in Oklahoma, the asymmetry of the outflows may be less critical operationally since pilots will tend to avoid penetrating such storms. However, asymmetry of low-altitude outflow is still a problem for detection of shears since asymmetric outflows have been identified within weak convective cells (Wilson et al., 1984).

With more investigation into downbursts it may be possible, using single Doppler radar data, to estimate the maximum shear with a given downburst and along which direction this shear is aligned. Perhaps this could be done using the two other Doppler moments (i.e., reflectivity and spectrum width). One possible way of determining the direction and strength of maximum outflow would be to use the reflectivity contours as a basis for determining which direction maximum outflow is orientated. From the cases in this study and the published microburst cases from JAWS (e.g., Wilson et al., 1984; Kessinger et al., 1983), it appears that the low altitude outflow most often takes on the shape of the reflectivity contours. For example, when the reflectivity contours are elliptical (or when the shape can be approximated by an ellipse) most often the strongest shears are nearly perpendicular to the major axis of the ellipse. If further study confirms that asymmetry in the reflectivity field is related to asymmetry of the outflow then knowledge of the radial shear measured across a downburst and the angle between the radial and the minor axis of the ellipse would allow estimation of the direction and extent of the maximum shear associated with the downburst.

Further study of downbursts is necessary if a single Doppler radar is to be used to identify downburst signatures so that wind shear along any intended flight path can be estimated and possibly forecasted for short periods of time.

References

Brown, R.A., C.R. Safford, S.P. Nelson, D.W. Burgess, W.C. Bumgarner, M.L. Weible, and L.C. Forner, 1981: Multiple Doppler radar analysis of severe thunderstorms: Designing a general analysis system. NOAA Tech. Memo. ERL NSSL-92, National Severe Storms Laboratory, Norman, OK (NTIS #PB82-114117), 18 pp.

Byers, H.R. and R.R. Braham, 1949: The Thunderstorm, U.S. Weather Bureau, Washington, D.C., 287 pp.

Cressman, G.P., 1959: An operational objective analysis system. Mon. Wea. Rev., 87, 367-374.

Darkow, G.L., 1969: An analysis of over sixty tornado proximity soundings. Proc. Sixth Conf. on Severe Local Storms, Amer. Meteor. Soc., 148-151.

Davies-Jones, R.P., 1979: Dual-Doppler radar coverage area as a function of measurement accuracy and spatial resolution. J. Appl. Meteor., 18, 1229-1233.

Emanuel, T.K., 1981: A similarity theory for unsaturated downdrafts within clouds. J. Atmos. Sci., 38, 1541-1580.

Forbes, G.S. and R.M. Wakimoto, 1983: A concentrated outbreak of tornadoes, downbursts and microbursts, and implications regarding vortex classifications. Mon. Wea. Rev., 111, 220-235.

Frost, W., 1983: Flight in low-level wind shear. NASA Contractor Report 3678, 107 pp.

Fujita, T.T., 1978: Manual of Downburst Identification for Project NIMROD. SMRP Research Paper 156, University of Chicago, 104 pp.

Fujita, T.T., 1981: Tornado and downbursts in the context of generalized planetary scales. J. Atmos. Sci., 38, 1511-1534.

Fujita, T.T., 1985: The Downburst: Microburst and Macroburst. SMRP Research Paper 210, University of Chicago, 122 pp.

Fujita, T.T., and R.M. Wakimoto, 1983: Microbursts in JAWS depicted by Doppler radars, PAM, and aerial photographs. Preprints, 21st Conference on Radar Meteorology, Amer. Meteor. Soc., 638-645.

Haman, K.E., and M. Niewiadomski, 1980: Cold downdrafts in cumulonimbus clouds. Tellus, 32, 525-536.

Kamburova, P.L., and F.H. Ludlam, 1966: Rainfall evaporation in thunderstorm downdrafts. Quart. J. Roy. Meteor. Soc., 92, 510-518.

Klemp, J.B., and R. Rotunno, 1983: A study of the tornadic region within a supercell thunderstorm. J. Atmos. Sci., 40, 359-377.

Klemp, J.B., and R.B. Wilhelmson, 1978: Simulations of right and left-moving storms through storm splitting. J. Atmos. Sci., 35, 1097-1110.

Klingle, D.L., 1985: A gust front case studies handbook. Project Report ATC-129, Lincoln Laboratory, Lexington, MA, 108 pp.

Knupp, K.R., 1985: Precipitating convective cloud downdraft structure: A synthesis of observations and modeling. Ph.D. Dissertation, Colorado State University, 296 pp.

Lemon, J.R., R.J. Donaldson, D.W. Burgess, and R.A. Brown, 1977: Doppler radar application to severe thunderstorm study and potential real-time warning. Bull. Am. Meteor. Soc., 58, 1187-1193.

Lemon, J.R., and C.A. Doswell, 1979: Severe thunderstorm evolution and mesocyclone structure as related to tornadogenesis. Mon. Wea. Rev., 107, 1184-1197.

Mahapatra, P.R., and J.T. Lee, 1984: The role of NEXRAD in aircraft navigation and flight safety enhancement. J. Inst. Navig., 31(1), 21-37.

Mahapatra, P.R., D.S. Zrnic', and R.J. Doviak, 1983: Optimum siting of NEXRAD to detect hazardous weather at airports. J. Aircr. 20 (4) 363-371.

Marwitz, J.D., 1972: The structure and motion of severe hailstorms. Part I: Supercell storms. J. Appl. Meteor. 11, 166-179.

McCarthy, J., and V. Norviel, 1982: Numerical and flight simulator test of the flight deterioration concept. NASA Contractor Report 3500, NASF-33458, Marshall Space Flight Center, AL, 31 pp.

McCarthy, J., and J.W. Wilson, 1984: The microburst as a hazard to aviation: structure, mechanisms, climatology, and nowcasting. Preprints Nowcasting II Symposium, Norrkoping, Sweden, 2-7 Sept.,ESA 51-208, 21-30.

McCarthy, J., J.W. Wilson, and T.T. Fujita, 1982: The joint airport weather studies project. Bull. Amer. Meteor. Soc., 63, 15-22.

NOAA, 1984: Storm Data., 26(5), 37-38.

National Research Council, 1983: Low-altitude wind shear and its hazard to aviation. National Academy Press, Washington, D.C., 112 pp.

Srivastava, R.C., 1985: A simple model of evaporatively driven downdraft: application to microburst downdraft. J. Atmos. Sci., 42, 1004-1023.

Wakimoto, R.M., 1983: The West Bend, Wisconsin, storm of 4 April 1981: A problem in operational meteorology. J. Clim. Appl. Meteor., 22, 181-189.

Wilson, J.W., R.D. Roberts, C. Kessinger, and J. McCarthy, 1984: Microburst wind structure and evaluation of Doppler radar for airport wind shear detection. J. Clim. Appl. Meteor., 23, 898-915.

Wolfson, M.D., 1983: Doppler radar observations of an Oklahoma downburst. M.S. Thesis, Massachusetts Institute of Technology, 99 pp.

Wolfson, M.D., J.T. Di Stefano, and T.T. Fujita, 1985: Low-altitude wind shear characteristics in the Memphis, TN area based on mesonet and LLWSAS data,. Preprints, 14th Conference on Severe Local Storms, Amer. Meteor. Soc., 326-327.

Zrnic' D.S., and J.T. Lee, 1983: Investigation of the detectability and lifetime of gust fronts and other weather hazards to aviation. FAA Report No. DOT/FAA/PM-83/33, 50 pp.

APPENDIX A

The Local - Environmental Check Algorithm

The local environmental check algorithm was developed to edit and unfold Doppler radar data automatically. It accomplishes this task by comparing a point in question with nine neighboring points; four in the same radial and five in the previous adjacent radial (Fig. A-1).

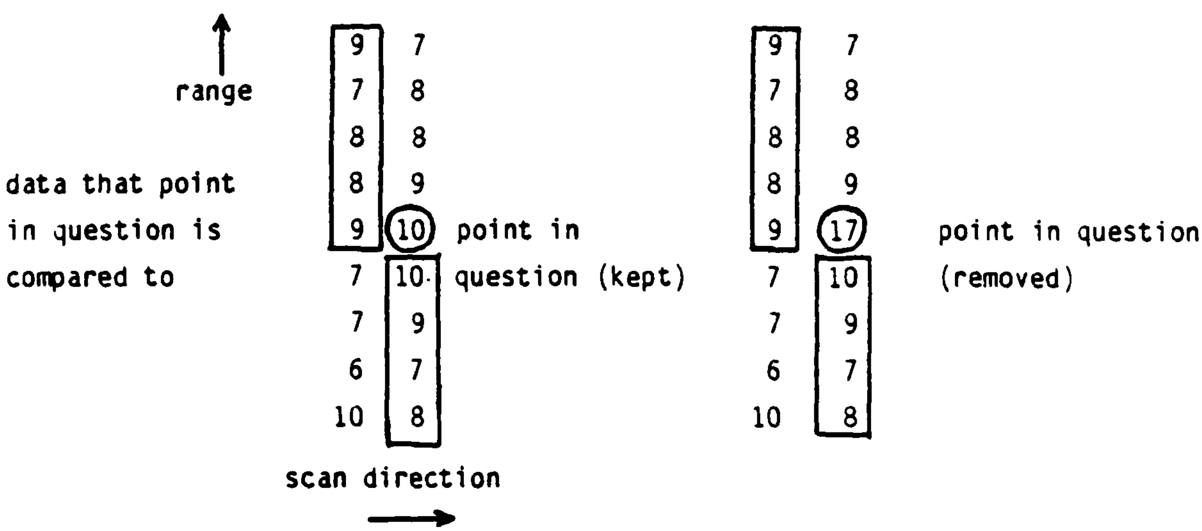

Fig. A-1. Example of radial velocity data. Data boxed in is nine points that the point in question is compared to.

Specifically, the algorithm compares the datum in question with the mean of nine neighboring points. If the datum value is within the mean ± a threshold, the datum is kept and the algorithm goes to the next point. The threshold is determined from the nature of the wind field. In an area with fairly small radial velocities and fairly laminar flow the threshold is set at 5 m/sec. In areas of larger radial velocities 40% of the mean of the neighboring points is used as the threshold value; and when the standard deviation of the neighboring points is large the threshold value is two times the standard deviation.

If the datum value in question is not within the mean ± the threshold of its nine neighboring points then an attempt to unfold the datum value into this range is completed. If unfolding is accomplished the algorithm continues on to the next data point.

If unfolding is not accomplished a final check is done to determine whether the point should be kept or removed. This final check uses the average of the four next (farther from the radar) points in the same radial. If the datum point is <u>not</u> within this mean ± the earlier computed threshold it is then removed. If it is within this range then one last attempt is made to fold the datum value using a slightly larger (user inputted) threshold value. If this is not possible the datum is then removed.

Because this algorithm uses different threshold values depending on the nature of the surrounding radial velocity field it is able to successfully edit data in areas of strong azimuthal and radial shear as well as in the clear air. Data used in the downburst cases presented in this report were edited using this algorithm.

APPENDIX B

Downburst Case 1 - 27 May 1984

The low-altitude outflow shown in Fig. 3a was associated with a cell located 33°/50 km from Norman at 1630 CST on this day. At this location the height of the radar beam was approximately 320 m AGL for the Norman radar and 420 m AGL for the Cimarron radar. Both data sets were interpolated to a grid with height 300 m. This cell was part of a line of thunderstorms that stretched east-west from the western Oklahoma border all the way to a point 120 km East-North-East of Norman at this time (Fig. B-1). The maximum reflectivity of this cell was 50 dBZ, which was one of the strongest cells in the line.

This line of thunderstorms had developed earlier in the day in the Northern part of Oklahoma and slowly moved to the SSE at a speed of ~5 m/sec. By midafternoon this line stretched east-west across the whole state of Oklahoma as well as into the Texas panhandle. Severe weather reports were numerous and widespread. When this line of thunderstorms passed through Norman, damaging outflow winds (38 m s^{-1}) and hail damage occurred.

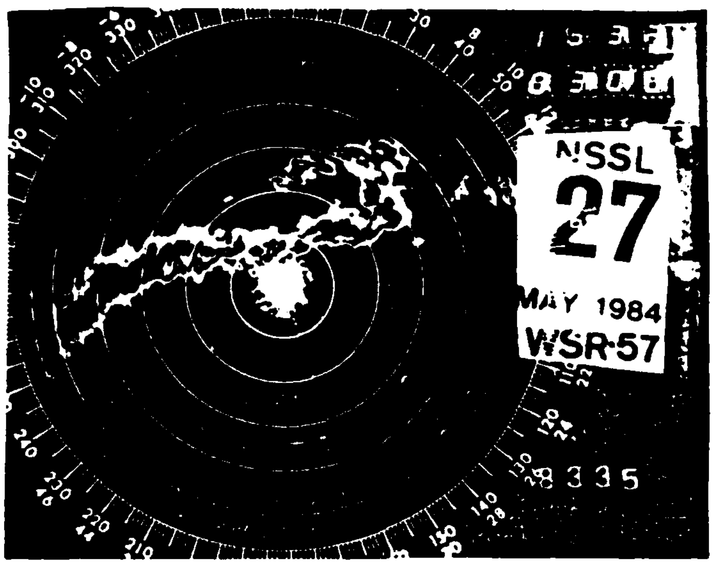

Fig. B-1. WSR-57 reflectivity field at 1630 CST showing line of thunderstorms. Range rings are at 40 km intervals. Elevation angle is 0.7°.

Downburst Case 2 - 19 May 1984

On 19 May 1984, a cell developed at 1330 CST ~ 60 km to the west of Norman. This storm moved slowly eastward (~7 m s^{-1}) and by 1430 CST had moved into the optimal dual Doppler coverage area for the two NSSL Doppler radars. The height of the radar beam for the Norman radar was approximately 170m and for the Cimarron radar the beam height was approximately 230 m. Data from both radars were interpolated to a grid with height 300 m. This storm was of fairly small size, ~10 km x 10 km, and moderate intensity (maximum reflectivity ~40 dBZ). At 1522 CST the first low-altitude divergence was noticed on the single Doppler display. The dual Doppler perturbation wind field at 1522:30 is shown in Fig. 4a. This low-altitude outflow is more symmetric, as well as weaker than the other two cases presented in this report. Figures B-2 and B-3 show perturbation wind fields at later times (1534 and 1541 respectively). Notice that there is still low-altitude divergence at both of these times although the wind fields are considerably different from the 1522 wind field and also different from each other. The initial downburst wind field is much more symmetric than in the later wind fields.

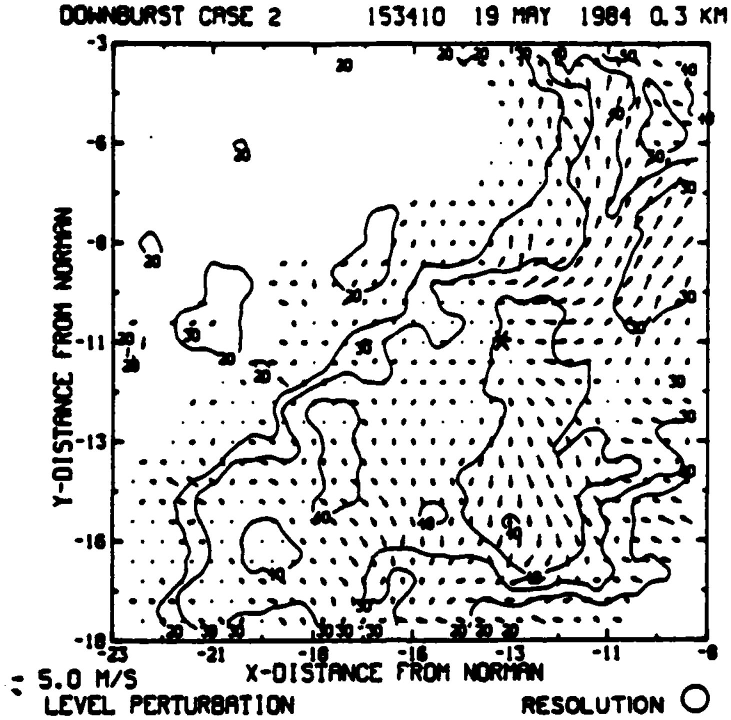

Fig. B-2. Same as Fig. 4a except at 153400 CST. Notice outflow is no longer symmetric.

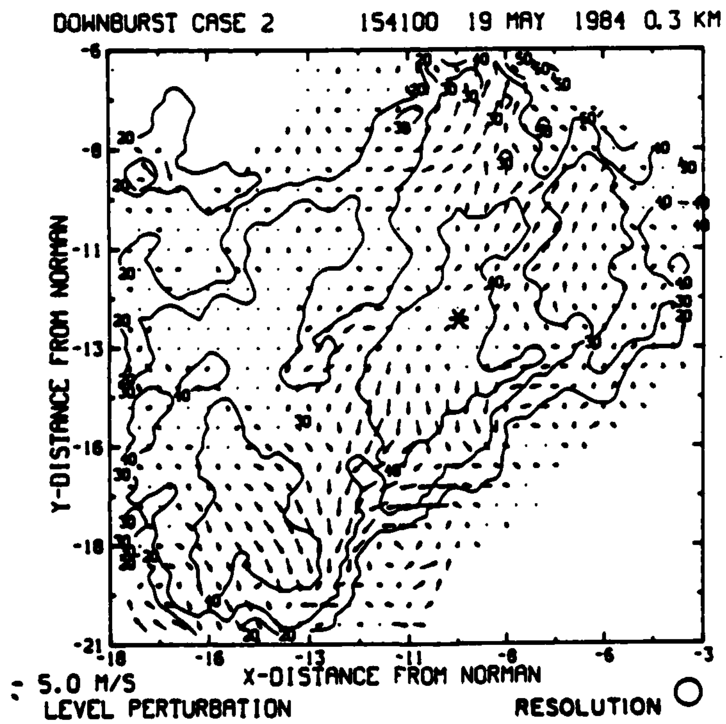

Fig. B-3. Same as Fig. 4a except at 154100 CST.

Downburst Case 3 - 19 June 1980

The downburst that occurred on 19 June 1980 in the dual Doppler radar area occurred in the Southwest quadrant of a storm in the vicinity of a core with reflectivity factor of 60 dBZ (Fig. 5a). The height of the radar beam of the Norman radar was approximately 550 m and the Cimarron beam was at 750 m. Data from both were interpolated to a grid with height 500 m. Figure B-4 is a 30 km x 70 km grid which shows the whole storm that was associated with the low-altitude divergence shown in Fig. 5a. There are actually two areas of divergence in this storm, the one shown in Fig. 5a and the one associated with the 50 dBZ core at (-24, -36) which is weaker. Reports of wind and hail damage were associated with this storm.

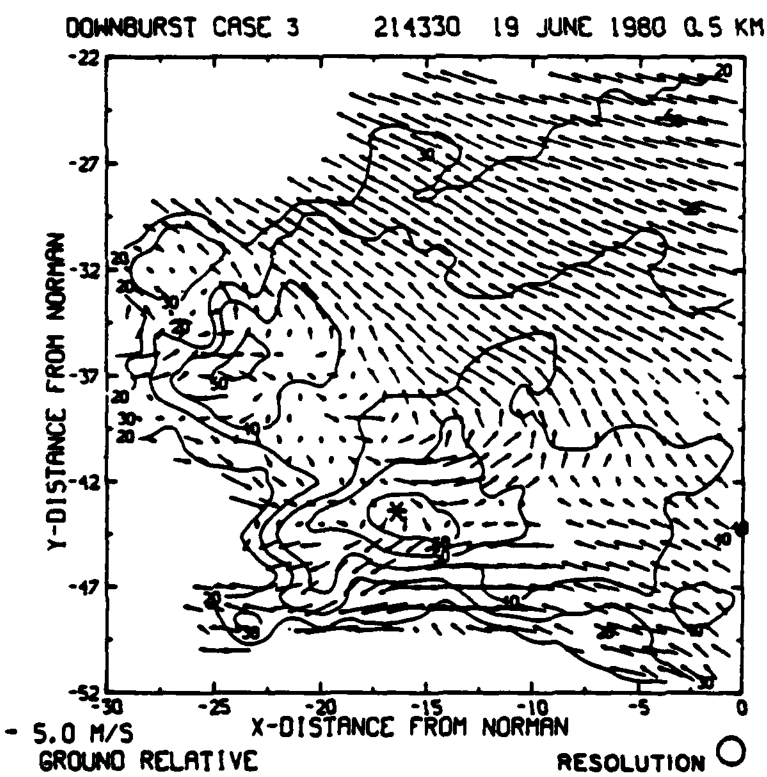

Fig. B-4. Dual Doppler vector wind field at 500 m AGL, 214330 CST, 19 June 1980. Data with elevation angle 0.5° was used from both radars and were interpolated to the 30 km x 30 km grid (dx = dy = 500 m) with a Cressman weight with horizontal radius of influence of 700 m. Contours are reflectivity in dBZ. Notice strong 60 dBZ core with divergence from it at (-15, -45).

APPENDIX C

Problems of Detecting Low-Altitude Divergence with Distant Radars

On 30 May 1982, a strong downburst occurred at 2007 CST ~ 75 km west of Norman. It appears that the low-level divergence associated with this downburst was detected by the Cimarron radar but not by the Norman radar. Figure C-1 is the contour plot of radial velocities at 2000 CST from the Cimarron radar. This is the time just before the downburst occurred. Figure C-2 is the contour plot of the downburst at its strongest time detected by the Cimarron radar (2007:45 CST). Notice the large change in the radial velocity field during this seven minutes. From a divergent field with weak gradients at 2000 CST to a strongly divergent field with strong gradients at 2007:45 CST. The height of the Cimarron beam at this range (~ 50 km) is 650 m with a vertical resolution of 650 m.

At the same time the Norman Doppler radar was scanning the same area. Figure C-3 and Figure C-4 are contour plots of the radial velocity field at 2000 CST and 2007 CST respectively, as observed by the Norman radar. Again, there is considerable change in the radial velocity fields with time but at neither time is there strong divergence. Instead, cyclonic shear is noticed which is similar to that seen in the mid-levels of the storm. The height of the Norman radar beam at this location was approximately 950 m with a vertical resolution of ~ 1150 m.

Although there was considerable overlap of the radar beams, the Norman Doppler beam weighted a higher part of the storm more strongly and thus it appears that the low-altitude divergence was not seen. It is possible that the different viewing angles of the Norman and Cimarron radar could account for some of the difference in radial velocities, however, it would take an

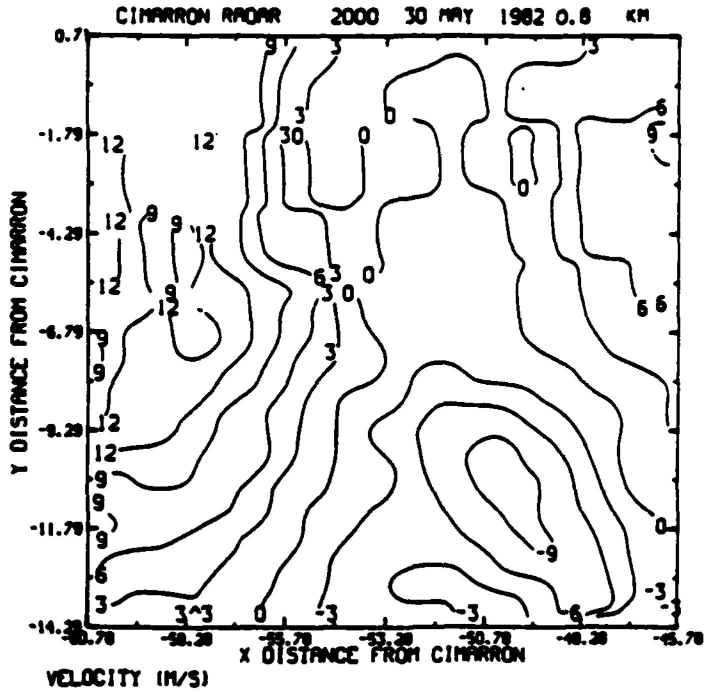

Fig. C-1. Cimarron radial velocity contour (interval 3 m s^{-1}) plot at 2000 CST, 30 May 1982. Some divergence is noticed at this time by the Cimarron radar.

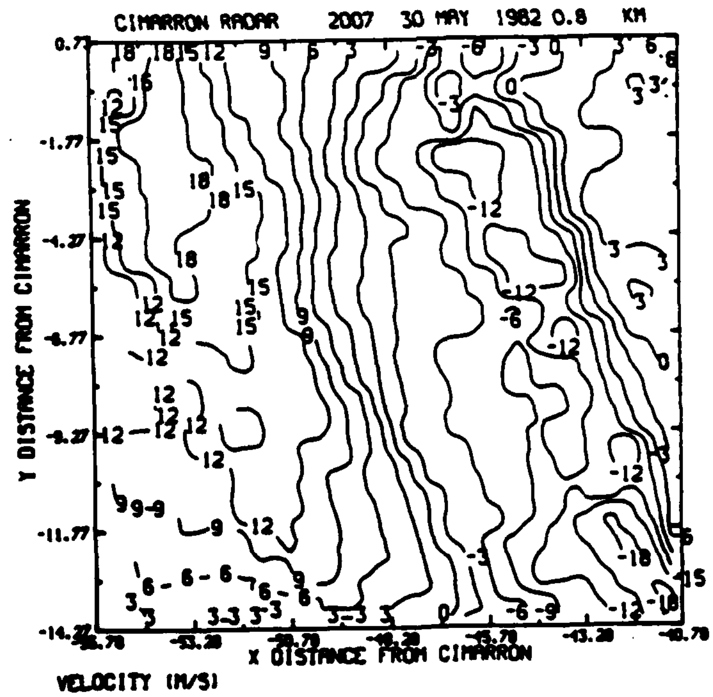

Fig. C-2. Same as C-1 except at 2007 CST. Notice the strong gradients at this time and the large change in the radial velocity fields between 2000 CST and 2007 CST.

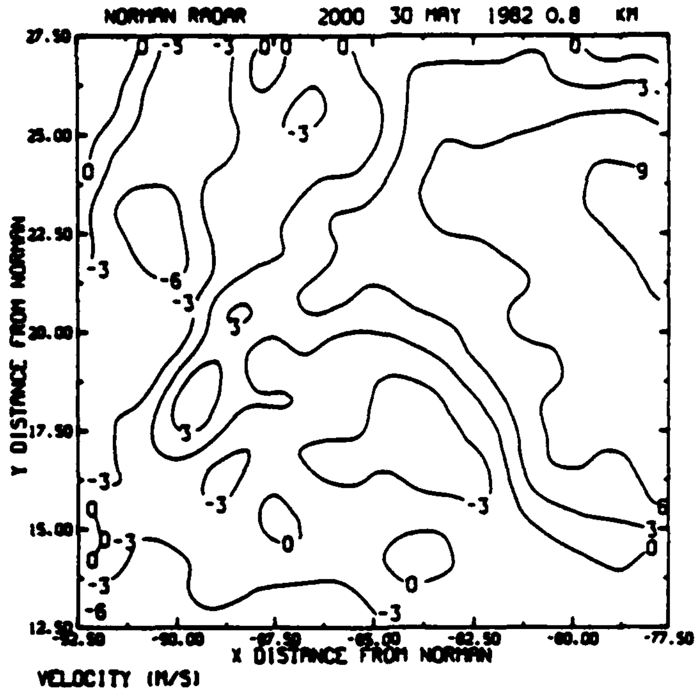

Fig. C-3. Norman radar radial velocity plot at 2000 CST, 30 May 1982 at same location as Figure C-1. Field is characterized by weak cyclonic shear.

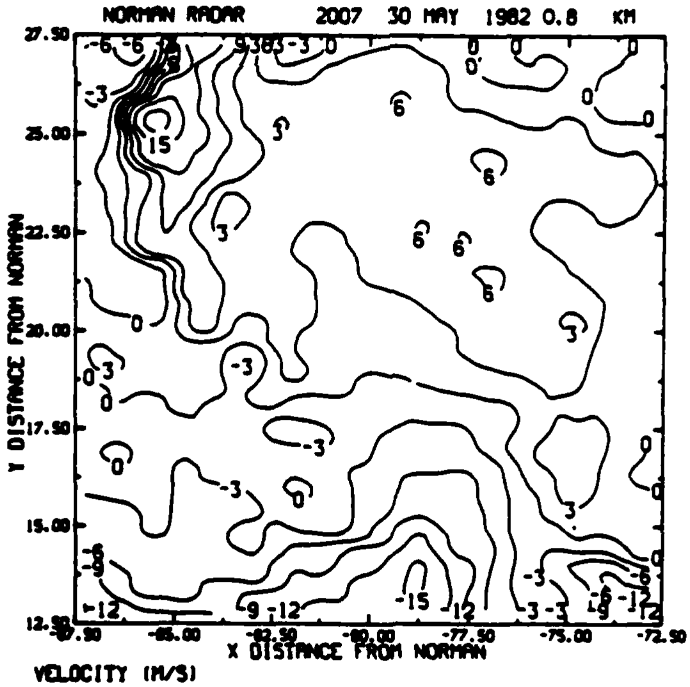

Fig. C-4. Same as Figure C-3 except at 2007 CST. Location is same as Figure C-2. Notice much stronger gradients and large change in radial velocity field between 2000 CST and 2007 CST. Also, little divergence is evident in the Norman data while strong divergence is evident in the Cimarron data at the same location.

unreasonably asymmetric case to account for all of this difference since the angle between the viewing angles was only ~20^0.

This case was a prime example of the difficulty in getting dual Doppler analysis of a downburst case. By the time that this downburst had moved close enough to the Norman radar so that the low-altitude divergence could be detected, the low-altitude divergence was weak and instead a strong gust front had ensued.

END

7-87

DTIC